KAPL-P-000197
(K97139)
CONF-980708--

OMVPE GROWTH OF GaInAsSb in the 2 to 2.4 um RANGE

G. W. Charache, C. A. Wang

December 1997

NOTICE

KAPL ATOMIC POWER LABORATORY SCHENECTADY, NEW YORK 13901

Operated for the U. S. Department of Energy
by KAPL, Inc. a Lockheed Martin company

DISCLAIMER

OMVPE Growth of GaInAsSb in the 2 to 2.4 μm Range*

C.A. Wang
Lincoln Laboratory, Massachusetts Institute of Technology, Lexington, MA 02173-9108

Abstract

$Ga_{1-x}In_xAs_ySb_{1-y}$ epilayers were grown lattice matched to GaSb substrates by organometallic vapor phase epitaxy using all organometallic precursors, which include triethylgallium, trimethylindium, tertiarybutylarsine, and trimethylantimony. Layers were grown over a temperature range between 525 and 575°C, a V/III ratio range between 0.9 and 1.7, $x < 0.2$ and $y < 0.2$, and on (100) GaSb substrates with 2° toward (100) or 6° toward (111)B. The overall material quality of these alloys depends on growth temperature, In content, V/III ratio, and substrate misorientation. A mirror-like surface morphology and room temperature photoluminescence (PL) could be obtained for GaInAsSb layers with peak emission in the wavelength range between 2 and 2.4 μm. Based on epilayer surface morphology and low temperature PL spectra, the crystal quality improves for growth temperature decreasing from 575 to 525°C, and with decreasing In content. In general, GaInAsSb layers grown on (100) GaSb substrates with a 6° toward (111)B misorientation exhibited smoother surfaces and narrower full width at half-maximum values of 4K PL spectra than layers grown on the more standard substrate (100) 2° toward (110). Nominally undoped GaInAsSb layers grown at 550°C are p-type with 300K hole concentration of ~5 x 10^{15} cm^{-3} and hole mobility of ~430 to 560 $cm^2/V\text{-}s$. The n- and p-type doping of GaInAsSb with diethyltellurium and dimethylzinc, respectively, are also reported.

*This work was sponsored by the Department of Energy under AF Contract No. F19628-95-C-0002. The opinions, interpretations, conclusions and recommendations are those of the author and are not necessarily endorsed by the United States Air Force.

1. Introduction

$Ga_{1-x}In_xAs_ySb_{1-y}$ is an important material for optoelectronic devices that operate in the mid-infrared. This alloy can be lattice matched to GaSb or InAs substrates and has a direct energy gap adjustable in the wavelength range from 1.7 (0.726 eV) to 4.2 μm (0.296 eV). Although most quaternary alloy compositions are predicted to exhibit thermodynamic immiscibility at typical growth temperatures [1,2], stable alloys with a cutoff wavelength of 2.39 μm have been grown by liquid phase epitaxy [3], and metastable alloys have been grown by organometallic vapor phase epitaxy (OMVPE) [4,5] and molecular beam epitaxy [6]. There have also been demonstrations of devices based on this alloy, which include lasers [7-9], photodetectors [10], and thermophotovoltaic devices [11,12]. Consequently, the technological interest of GaInAsSb continues to increase, especially for devices that operate in the wavelength range between 2 and 2.5 μm.

The energy gap dependence on composition of the $Ga_{1-x}In_xAs_ySb_{1-y}$ quaternary alloy, based on the binary bandgaps [13], is given by $E(x,y) = 0.726 - 0.961x - 0.501y + 0.08xy + 0.415x^2 + 1.2y^2 + 0.021x^2y - 0.62xy^2$. The energy gap is determined in large part by the In content of the alloy, while the As content mainly affects the lattice constant. For alloys lattice matched to GaSb, $y = 0.867(x)/(1 - 0.048x)$. OMVPE has been used to grow these alloys lattice matched to both InAs and GaSb substrates [4,5,14-17]. However, for the longer wavelength alloys, growth on GaSb substrates is preferred over InAs substrates due to thermodynamic considerations.

In previous reports on OMVPE growth of GaInAsSb, alloys were grown with trimethylgallium (TMGa) as the gallium precursor [4,5,14-16]. For growth temperatures which ranged between 500 and 550°C, TMGa was not completely pyrolized [4,15] and the composition of In in the alloy was found to be dependent on growth temperature. Although precursor decomposition is reactor and pressure dependent, we also determined from growth experiments of GaSb, that TMGa is only partially decomposed below 640°C. However, when triethylgallium (TEGa) is used, growth is mass-transport limited between 525 and 640°C [18].

Thus, there is a potential advantage to using TEGa as the gallium precursor for growth of GaInAsSb. In this paper, we report OMVPE growth of $Ga_{1-x}In_xAs_ySb_{1-y}$ alloys lattice matched to GaSb with TEGa, trimethylindium (TMIn), tertiarybutylarsine (TBAs), and trimethylantimony (TMSb). High quality epilayers lattice matched to GaSb substrates are obtained for alloys with room temperature cutoff wavelengths between 2 and 2.4 μm. Low temperature photoluminescence (PL) spectra show narrow near-bandedge transitions with full width at half-maximum (FWHM) values typically less than 10 meV, which is significantly lower than previous values reported for layers grown by OMVPE. We also report the n- and p-type doping of GaInAsSb using diethyltellurium (DETe) and dimethylzinc (DMZn), respectively.

2. Epitaxial Growth and Characterization

$Ga_{1-x}In_xAs_ySb_{1-y}$ epilayers were grown in a vertical rotating-disk reactor with H_2 carrier gas at a flow rate of 10 slpm and reactor pressure of 150 Torr [17]. Solution TMIn [19], TEGa, TBAs, and TMSb were used as organometallic precursors. Solution TMIn was selected to minimize source transients normally encountered when using the standard solid source TMIn [20]. On-line ultrasonic monitoring of the TMIn delivery confirmed that the output was stable over a several month period. TMIn and TEGa were maintained at 24°C, TMSb at 0°C, and TBAs at -8°C. For doping studies, DETe (10 ppm in H_2) and DMZn (1000 ppm in H_2) were used as n- and p-type doping sources, respectively. Precursors were premixed in a fast switching manifold before introduction into the reactor.

The total group III mole fraction was typically 3.5 to 4 x 10^{-4} which resulted in a growth rate of ~2.5 to 2.7 μm/h. The TMIn fraction in the gas phase, $p_{TMIn}/[p_{TMIn} + p_{TEGa}]$, was varied from 0.127 to 0.267 and the V/III ratio ranged from 0.9 to 1.7. For lattice matching to GaSb substrates, the TBAs fraction in the gas phase, $p_{TBAs}/[p_{TBAs} + p_{TMSb}]$, was varied from 0.05 to 0.15. Epilayers were grown at 525, 550, and 575°C.

$Ga_{1-x}In_xAs_ySb_{1-y}$ epilayers were grown without a GaSb buffer on (100) Te-doped GaSb substrates with various misorientations. The bulk of the layers were grown on substrates

misoriented 2° toward (110) or 6° toward (111)B. In a few experiments, (100) GaSb substrates with misorientations of 6° toward (110), 2° toward (111)A, 6° toward (111)A, or 2° toward (111)B were used. For direct comparison, an attempt was made to grow epilayers side-by-side on substrates of various misorientation angles to minimize the effects of run-to-run variability.

The surface morphology was examined using Nomarski contrast microscopy. Double-crystal x-ray diffraction (DCXD) was used to measure the degree of lattice mismatch $\Delta a/a$ to GaSb substrates. PL was measured at 4 and 300K using a PbS detector. The In and As content of epilayers was determined from DCXD splitting, the peak emission in 300K PL spectra, and the energy gap dependence on composition based on the binary bandgaps. For electrical characterization, GaInAsSb was grown at 550°C on semi-insulating (SI) (100) GaAs substrates misoriented 2° toward (110) or 6° toward (111)B. Since the mismatch between GaInAsSb and GaAs is ~8%, a GaSb buffer layer of various thicknesses was first grown at 550°C to reduce the contribution of electrically active defects due to the lattice mismatch. Carrier concentration and mobility of GaInAsSb epilayers, which were grown about 3 μm thick, were obtained from Hall measurements based on the van der Pauw method.

3. Results and discussion

3.1 Surface morphology

The surface morphology of GaInAsSb layers depends on V/III ratio, substrate misorientation, In content, and growth temperature. Figure 1 shows the surface morphology of $Ga_{0.88}In_{0.12}As_{0.1}Sb_{0.9}$ layers grown with various V/III ratios at 575°C on (100) GaSb substrates misoriented 2° toward (110). The layers are nominally lattice matched to the GaSb substrate ($\Delta a/a < 1.5 \times 10^{-3}$). For V/III = 0.9, the surface is metal-rich and hazy to the naked eye. When the V/III ratio was increased to 1.05, the surface morphology is mirror-like. As the V/III ratio was increased further, however, Nomarski contrast microscopy revealed surface texture which increases with V/III ratio. These results are similar to the morphology dependence on V/III ratio observed for GaSb [18]. When the growth temperature was reduced to 550 and 525°C, the

minimum V/III ratio increased to 1.15 and 1.25, respectively. We also observed that GaInAsSb layers of similar composition exhibit a smoother morphology when grown at a lower temperature of 550 or 525°C compared to 575°C.

The surface morphology was also found to be dependent on substrate misorientation. Figures 2a-f are Nomarski interference micrographs of $Ga_{0.82}In_{0.18}As_{0.15}Sb_{0.85}$ layers grown at 550°C and V/III = 1.25 on (100) GaSb substrates with a 2 or 6° misorientation toward (110), (111)A, and (111)B, respectively. The layers grown on substrates with a 2° misorientation exhibit considerable texture. A smoother surface morphology is observed for layers grown on substrates with a 6° misorientation, and the smoothest surface is observed for 6° toward (111)B misorientation.

The In content affects the surface morphology of epilayers grown on (100) substrates with a 2° toward (110) misorientation. As the In concentration decreases (i.e., composition moving away from the GaSb corner of the miscibility phase diagram [4]), the surface becomes smoother, and for $Ga_{0.9}In_{0.1}As_{0.08}Sb_{0.92}$, a mirror smooth surface is obtained for epilayers grown at a growth temperature of 550°C. In general, these observations suggest that the 6° toward (111)B misorientation provides a wider operating range of growth parameters for obtaining a smooth morphology, and that surface morphology improves at lower growth temperatures.

3.2 Alloy composition control

As discussed above, the energy gap of $Ga_{1-x}In_xAs_ySb_{1-y}$ depends on both the x- and y-value, but is more strongly affected by the x-value, while the y-value is used to adjust the lattice constant to match to the GaSb substrate. The distribution coefficients of In and As are shown in Figs. 3a and 3b, respectively. Test data are plotted for layers grown on (100) 2° toward (110) substrates. The growth temperature was 525, 550, or 575°C, and the V/III ratio ranged between 1.1 and 1.3. For these layers, $|\Delta a/a| < 2 \times 10^{-3}$. At 525°C, the In distribution coefficient is 1.2, and decreases to 0.95 and 0.5 at 550 and 575°C, respectively. The trend of a lower In

distribution coefficient with increasing temperature is similar to results reported for growth using TMGa and TMIn [4,15]. However, in those studies, the dependence is attributed to the increase in TMGa pyrolysis with temperature. For the range of growth temperatures and reactor used in this study, it is likely that both TMIn and TEGa are completely pyrolyzed. Thus, these results are somewhat surprising and may reflect a difference in surface kinetics.

Figure 3b shows that the As distribution coefficient is approximately unity independent of growth temperature, indicating complete pyrolysis of TBAs and TMSb. This result is somewhat surprising since we concluded from growth studies of GaSb with TEGa and TMSb, that a temperature of 600°C is required to completely pyrolyze TMSb in the vertical reactor used in this study [18]. The decomposition of TMSb may be enhanced by the presence of the other precursors used in this study. In contrast, the As distribution coefficient was reported to be a strong function of temperature when TMGa, TMIn, TBAs, and TMSb were used as precursors [15].

The degree of lattice mismatch of GaInAsSb epilayers on GaSb can influence the performance of minority carrier-type devices, such as thermophotovoltaics [12]. Therefore, we determined the sensitivity of lattice mismatch on the fraction of TBAs in the gas phase. Since the As distribution coefficient is unity, the sensitivity is not temperature dependent. The lattice mismatch variation is about 1.5×10^{-3} % per TBAs mole fraction in the gas phase, which corresponds to about 160 to 180 arc sec per sccm H_2 flow through the TBAs bubbler for group III mole fraction of 4×10^{-4}. Since the reproducibility of a typical mass flow controller is 0.1 sccm, the data indicate that TBAs can be used to provide excellent controllability of lattice-matching conditions. The FWHM of the peak of a typical DCXD scan for a 2-μm-thick $Ga_{0.9}In_{0.1}As_{0.08}Sb_{0.92}$ layer is 21 arc sec, which is comparable to the 22 arc sec FWHM for the GaSb substrate. When the lattice mismatch is greater than about 5×10^{-3}, a cross-hatch surface morphology is observed.

3.3 Optical properties

Photoluminescence spectra measured at 4K of GaInAsSb layers grown at 550°C on (100) GaSb substrates with either a 2° toward (110) or 6° toward (111)B misorientation are shown in Fig. 4. The FWHM is 15.4 meV for layer A, with a 2° toward (110) misorientation, compared to a FWHM of 7.5 meV for layer B, with the 6° toward (111)B misorientation. In addition, the peak emission is slightly longer at 2045 nm for layer A compared to 1995 nm for layer B. The PL spectra measured at room temperature also show a longer peak emission for layer A at 2236 nm compared to 2217 nm for layer B. This difference corresponds to a small decrease in In content from about 0.142 to 0.139.

Table 1 lists PL data for lattice-matched GaInAsSb layers of various alloy compositions grown at 525 and 550°C, and indicates similar trends. The FWHM values are lower and the PL peak position is at shorter wavelength for the 6° toward (111)B misorientation compared to the 2° toward (110) misorientation. A dependence of In incorporation on substrate misorientation has also been reported for InGaAs [21]. However, in the present study, the misorientation angles and directions are different, so a possible mechanism for the observed In dependence cannot be suggested. In addition, the data in Table 1 suggest that FWHM values are dependent on growth temperature. Narrower FWHM values are obtained for GaInAsSb grown on (100) 2° toward (110) substrates when grown at 525°C compared to 550°C. For most of the layers, the difference in PL peak energy at 4 and 300K is in the range between 0.05 and 0.07 meV, which is in line with the energy difference of the near-bandedge transitions for GaSb [22] and InAs [23]. The PL peak position is at a longer wavelength at 4K compared to 300K for sample 392a. Since the FWHM value is large, it is more likely that the peak is related to an impurity transition.

Figure 5 summarizes our best FWHM data for GaInAsSb epilayers. These samples were grown at 550°C on (100) 6° toward (111)B substrates or at 525°C on either (100) 2° toward (110) or 6° toward (111)B substrates. Also shown for comparison are data for layers grown by OMVPE on (100) substrates [5,15]. The FWHM values decrease with increasing PL peak

energy. Our FWHM values are significantly smaller than those reported previously, especially for samples at lower PL peak energy. The smallest FWHM value measured is 7.1 meV at 0.606 eV. Our FWHM values are comparable to those reported for layers grown by MBE [11]. For GaInAsSb grown by LPE, a FWHM value of 9 meV at 0.587 eV (2112 nm) was reported [24].

3.4 Electrical properties

The carrier concentration and mobility were measured from GaInAsSb layers grown on SI GaAs substrates because SI GaSb substrates are not available. Since the lattice mismatch between GaInAsSb (lattice matched to GaSb) and GaAs is 8%, misfit dislocations are generated and propagate through the GaInAsSb epilayer [25,26]. These defects can be electrically active [27-29], but can be mitigated by the growth of a buffer layer [28,29]. For evaluations performed in this study, a GaSb buffer layer was first grown on the GaAs substrate at 550°C at a growth rate of ~1 μm/h.

3.4.1 Undoped GaInAsSb

The electrical properties measured at 300K of nominally undoped $Ga_{0.84}In_{0.14}As_{0.12}Sb_{0.88}$ layers grown at 550°C are shown in Fig. 6 as a function of GaSb buffer layer thickness. SI GaAs substrates (100) 2° toward (110) were used. All layers are p-type with hole concentration (mobility) decreasing (increasing) with GaSb buffer layer thickness. Without a buffer layer, the hole concentration is as high as 5 x 10^{16} cm^{-3}, and decreases by an order of magnitude when the buffer layer is 0.4 μm or greater. The mobility is as low as 90 cm^2/V-s without the buffer compared to 430 and 560 cm^2/V-s with a 0.4 and 0.8-μm-thick GaSb buffer layer, respectively. The residual hole concentration is almost 2 times lower than that for our GaInAsSb layers grown at 575°C [17]. Considerably higher hole concentration (2 to 5 x 10^{16} cm^{-3}) and lower hole mobility (220 to 320 cm^2/V-s) values were recently reported for GaInAsSb grown with TMGa, TMIn, arsine, and TMSb [29]. For GaInAsSb layers grown by

MBE, the hole concentration was reported to be 4 to 5 x 10^{16} cm^{-3} and mobility to be 254 cm^2/V-s [30].

3.4.1 n- and p-Type Doping

For doping studies, $Ga_{0.87}In_{0.13}As_{0.12}Sb_{0.88}$ layers were grown on a 0.4-μm-thick undoped GaSb buffer layer on SI GaAs substrates, (100) 2° toward (110) or (100) 6° toward (111)B. Figures 7a and 7b show results plotted as a function of the dopant mole fraction for p- and n-type layers, respectively. The hole concentration ranges from 6.3 x 10^{16} cm^{-3} to 1.7 x 10^{18} cm^{-3} for DMZn mole fraction 7.5 to 80 x 10^{-7}. It is 1.5 to 1.6 times greater for layers grown on (100) substrates with a 6° toward (111)B misorientation compared to the 2° toward (110) misorientation. These results suggest that there is a preferential incorporation of Zn for the 6° toward (111)B misorientation. For n-type GaInAsSb, the electron concentration ranges from 2.3 x 10^{17} cm^{-3} to 2.3 x 10^{18} cm^{-3} for DETe mole fraction 5 to 80 x 10^{-9}, and is 0.86 to 0.9 times lower for the 6° toward (111)B misorientation compared to the 2° toward (110) misorientation.

The 300K electrical properties of p- and n-doped $Ga_{1-x}In_xAs_ySb_{1-y}$ (x~0.13, y~0.12) are summarized in Figs. 8a and 8b, respectively. With one exception, the data are plotted for GaInAsSb grown on a 0.4-μm-thick buffer layer (see Fig. 8a). The hole concentration ranges from 4.4 x 10^{15} to 1.7 x 10^{18} cm^{-3} with mobility values between 560 and 180 cm^2/V-s, respectively. The electron concentration ranges from 2.3 x 10^{17} to 2.3 x 10^{18} cm^{-3}, with corresponding mobility values between 5208 and 2084 cm^2/V-s, respectively. The mobility values are likely to be an underestimate of true values, since the mismatch is significant, and we have not tried to optimize the GaSb buffer layer growth. Although there is extremely limited data for GaInAsSb electrical properties [5,17,29,30], we believe these results are a significant improvement over results reported previously.

4. Conclusions

GaInAsSb layers were grown by OMVPE using TEGa, TMIn, TBAs, and TMSb at 525, 550, and 575°C. The In distribution coefficient is temperature dependent, while the As distribution coefficient is temperature independent. The surface morphology of these layers depends on V/III ratio, substrate misorientation, growth temperature, and alloy composition. Mirror-smooth surface morphology could be obtained for alloys with cutoff wavelengths between 2 and 2.4 μm. For GaInAsSb grown on (100) 2° toward (110) GaSb substrates, the surface morphology and low temperature PL properties improve when the growth temperature is reduced from 575°C to 550 and 525°C. Reducing the In content also improves morphology. GaInAsSb epilayers grown on (100) 6° toward (111)B GaSb substrates have superior morphology and PL properties compared to layers grown on (100) 2° toward (110) GaSb substrates. The FWHM values of 4K PL spectra are lower than values previously reported and the smallest value measured is 7.1 meV at 0.606 eV. The electrical properties of GaInAsSb were measured for layers grown on SI GaAs substrates. Incorporation of a GaSb buffer layer improves the electrical properties and GaInAsSb layers containing a GaSb buffer layer of 0.4-μm-thick or greater have a hole concentration of ~5 x 10^{15} cm^{-3} and hole mobility of ~ 430 to 560 $cm^2/V\text{-}s$. GaInAsSb was doped p-type in the range 10^{16} to 10^{18} cm^{-3} with DMZn, and n-type in the range 10^{17} to 10^{18} cm^{-3} with DETe.

Acknowledgments

The authors gratefully acknowledge D.R. Calawa for x-ray diffraction, J.W. Chludzinski for photoluminescence, R.J. Poillucci and D.C. Oakley for technical assistance, K.J. Challberg for manuscript editing, and D.L. Spears and B-Y. Tsaur for continued support and encouragement.

References

1. K. Onabe, Jpn. J. Appl. Phys. 21 (1982) 964.
2. G.B. Stringfellow, J. Cryst. Growth 58 (1982) 194.
3. E. Tournie, F. Pitard, and A. Joullie, J. Cryst. Growth 104 (1990) 683.
4. M.J. Cherng, H.R. Jen, C.A. Larsen, G.B. Stringfellow, H. Lundt, and P.C. Taylor, J. Cryst. Growth 77 (1986) 408.
5. J. Shin, T.C. Hsu, Y. Hsu, and G.B. Stringfellow, J. Cryst. Growth 179 (1997) 1.
6. H.K. Choi, S.J. Eglash, and G.W. Turner, Appl. Phys. Lett. 64 (1994) 2474.
7. D.Z. Garbuzov, R.U. Martinelli, H. Lee, P.K. York, R.J. Menna, J.C. Connolly and S.Y. Narayan, Appl. Phys. Lett. 69 (1996) 2006.
8. H.K. Choi, G.W. Turner, M.K. Connors, S. Fox, C. Dauga, and M. Dagenais, IEEE Photon. Technol. Lett. 7 (1995) 281.
9. C.A. Wang and H.K. Choi, Appl. Phys. Lett. 70 (1997) 802.
10. Y. Shi, J.H. Zhao, H. Lee, J. Sarathy, M. Cohen, and G. Olsen, Electron. Lett. 32 (1996) 2268.
11. P.N. Uppal, G. Charache, P. Baldasaro, B. Campbell, S. Loughin, S. Svensson, and D. Gill, J. Cryst. Growth 175/176 (1997) 877.
12. C.A. Wang, H.K. Choi, G.W. Turner, D.L. Spears, M.J. Manfra, and G.W. Charache, in 3rd NREL Conference on the Thermophotovoltaic Generation of Electricity, edited by J.P. Benner and T.J. Coutts, AIP Conference Proceedings Vol. 401, Woodbury, NY, 1997, p. 75.
13. J.C. DeWinter, M.A. Pollock, A.K. Srivastava, and J.L. Zyskind, J. Electron. Mater. 14 (1985) 729.
14. A. Giani, J. Bougnot, F. Pascal-Delannoy, G. Bougnot, J. Kaoukab, G.G. Allogho, and M. Bow, Mater. Sci. Eng. B9 (1991) 121.
15. M. Sopanen, T. Koljonen, H. Lipsanen, and T. Tuomi, J. Cryst. Growth 145 (1994) 492.
16. S. Li, Y. Jin, T. Zhou, B. Ahang, Y. Ning, H. Jiang, G. Yuan, X. Zhang, and J. Yuan, J. Cryst. Growth 156 (1995) 39.
17. C.A. Wang, G.W. Turner, M.J. Manfra, H.K. Choi, and D.L. Spears, Mater. Res. Soc. Symp. Proc. 450 (1997) 55.
18. C.A. Wang, S. Salim, K.F. Jensen, and A.C. Jones, J. Cryst. Growth 170 (1997) 55.
19. D.M. Frigo, G.P.M. van Mier, J.H. Wilkie, and A.W. Gal, Appl. Phys. Lett. 61 (1992) 531.
20. B.R. Butler and J.P. Stagg, J. Cryst. Growth 94 (1989) 481.

21. J. te Nijenhuis, P.R. Hageman, and L.J. Giling, J. Cryst. Growth 167 (1996) 397.

22. S.C. Chen and Y.K. Su, J. Appl. Phys. 66 (1989) 350.

23. Z.M. Fang, K.Y. Ma, D.H. Jaw, R.M. Cohen, and G.B. Stringfellow, J. Appl. Phys. 67 (1990) 7034.

24. E. Tournie, J.-L. Lazzari, F. Pitard, C. Alibert, A. Joullie, and B. Lambert, J. Appl. Phys. 68 (1990) 5936.

25. R.E. Mallard, P.R. Wilshaw, N.J. Mason, P.J. Walker, and G.R. Booker, Inst. Phys. Conf. Ser. 100 (1989) 331.

26. J.M. Kang, M. Nouaoura, L. Lassabatere, and A. Rocher, J. Cryst. Growth 143 (1994) 115.

27. B.J. Baliga and S.K. Ghandi, J. Electrochem. Soc. 121 (1974) 1646.

28. S. Kalem, J.I. Chyi, H. Morkoc, R. Bean, and K. Zanio, Appl. Phys. Lett. 53 (1988) 1647.

29. A. Giani, F. Pascal-Delannoy, J. Podlecki, and G. Bougnot, Mater. Sci. Eng. B41 (1996) 201.

30. A.Z. Li, J.Q. Zhong, Y.L. Zheng, J.X. Wang, G.P. Ru, W.G. Bi, and M. Qi, J. Cryst. Growth 150 (1995) 1375.

Figure Captions

Figure 1 Surface morphology of GaInAsSb epilayers grown on (100) GaSb substrates misoriented 2° toward (110) at 575°C and various V/III ratios.

Figure 2 Surface morphology of GaInAsSb epilayers grown at 550°C on (100) GaSb substrate with various substrate misorientations and V/III ratio of 1.25.

Figure 3 Distribution coefficients of (a) In and (b) As for GaInAsSb grown nominally lattice matched to GaSb at 525°C (open squares), 550°C (solid circles), and 575°C (open circles). Data plotted for layers grown on (100) 2° toward (110) GaSb substrates and V/III ratio range between 1.1 and 1.3.

Figure 4 Photoluminescence spectra measured at 4K of GaInAsSb grown on (100) 2° toward (110) GaSb substrates, layer A, and (100) 6° toward (111)B, layer B. Layers were grown at 550°C.

Figure 5 Photoluminescence FWHM measured at 4K of GaInAsSb layers grown on GaSb substrates. Solid circles this work, open squares from reference 15, and open triangle from reference 5.

Figure 6 Electrical properties measured at 300K of nominally undoped $Ga_{0.86}In_{0.14}As_{0.12}Sb_{0.88}$ grown at 550°C as a function of GaSb buffer layer thickness.

Figure 7 Doping studies for (a) p-GaInAsSb and (b) n-GaInAsSb grown at 550°C. Concentration measured at 300K for layers grown on (100) semi-insulating GaAs substrates with 2° toward (110) misorientation (closed circles) and 6° toward (111)B misorientation (open circles).

Figure 8 Electrical properties measured at 300K of (a) p-$Ga_{0.87}In_{0.13}As_{0.12}Sb_{0.88}$ and (b) n-$Ga_{0.87}In_{0.13}As_{0.12}Sb_{0.88}$. Closed circles represent data with 0.4-μm-thick GaSb buffer layer. Open circle for 0.8-μm-thick buffer layer.

Table 1. Photoluminescence of GaInAsSb

Sample	4K PL peak (nm)	300K PL peak (nm)	4K FWHM (meV)	Growth temp (°C)	Substrate misorientation
404a	2082	2296	11.2	525	2°(110)
404b	2042	2276	9.5	525	6°(111)B
413	2030	2263	8.1	525	2°(110)
416b	2047	2267	7.1	525	6°(111)B
392a	2432	2396	45	550	2°(110)
391b	2138	2355	16.4	550	6°(111)B
396a	1875	2100	15.4	550	2°(110)
396b	1865	2080	9.6	550	6°(111)B

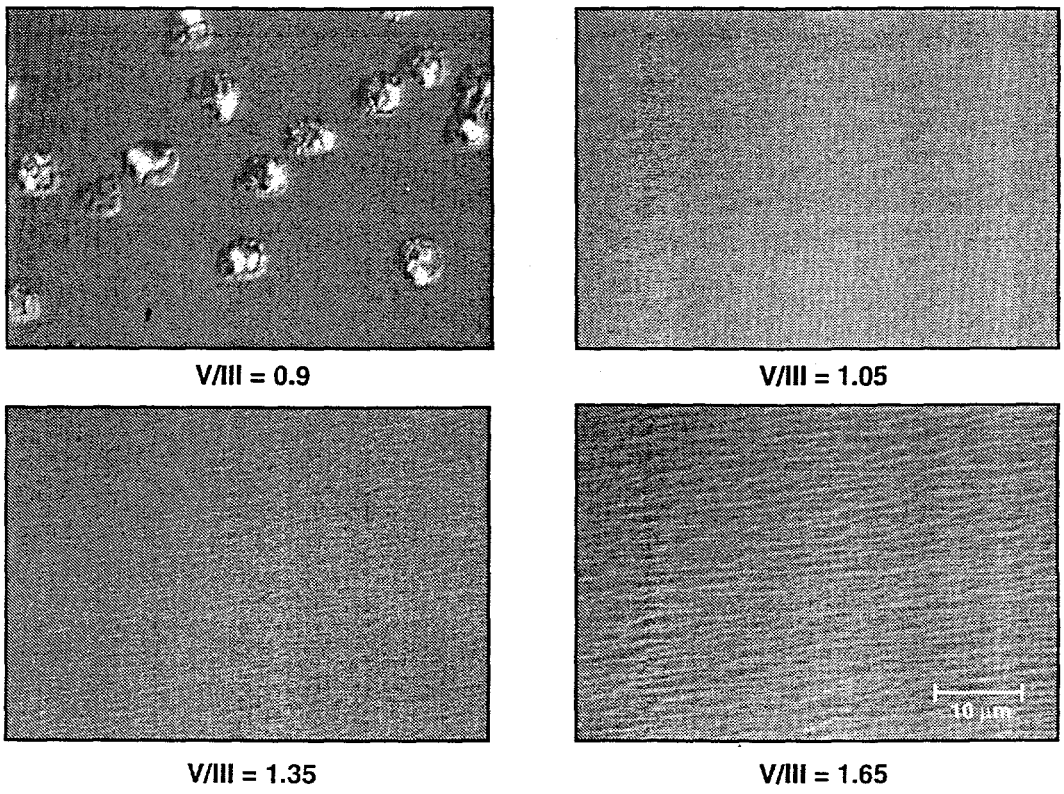

Figure 1

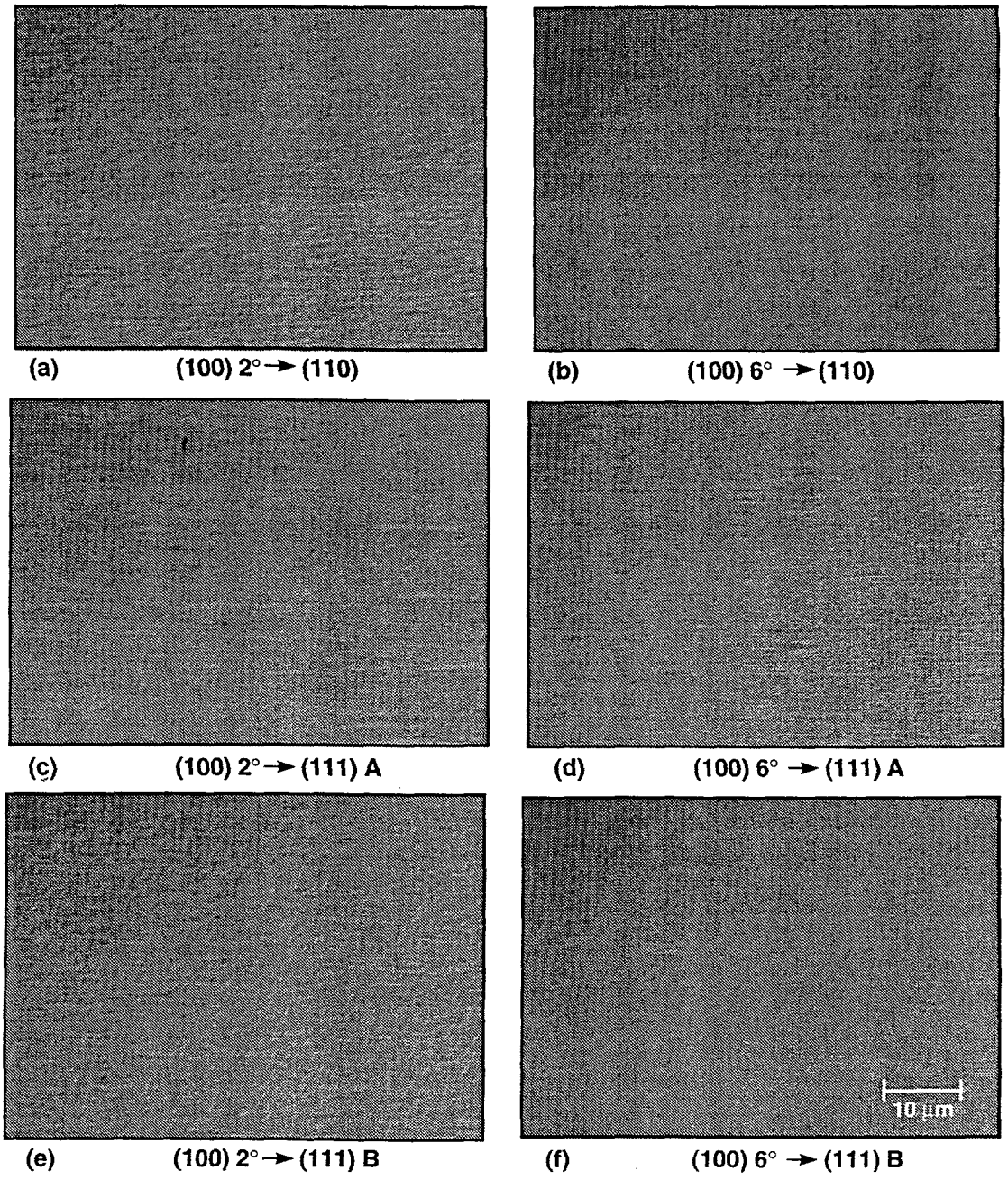

Figure 2

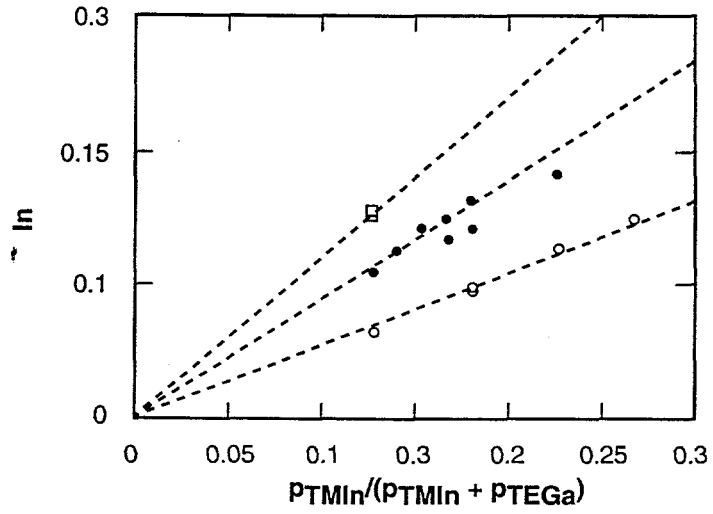

304549-6

Figure 3a

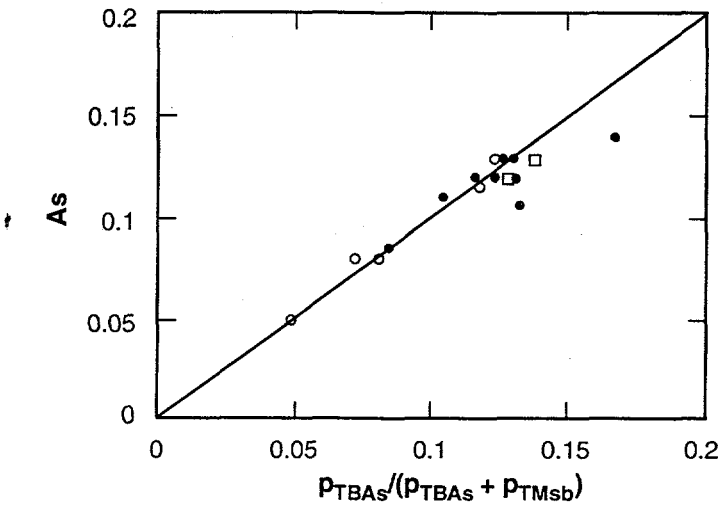

304549-5

Figure 3b

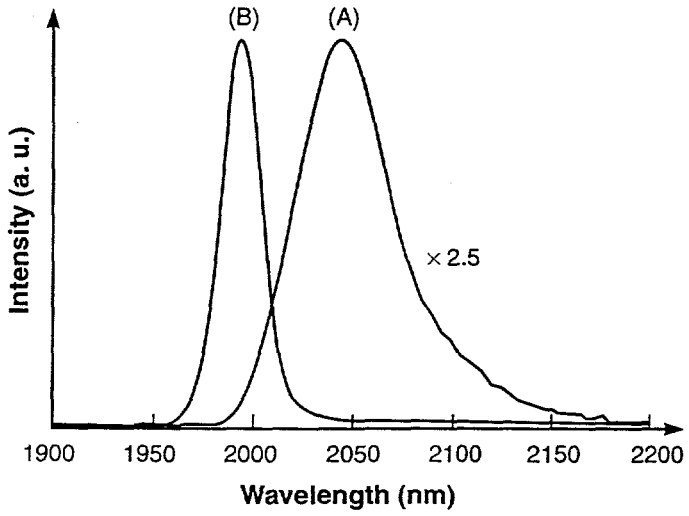

304549-12

Figure 4

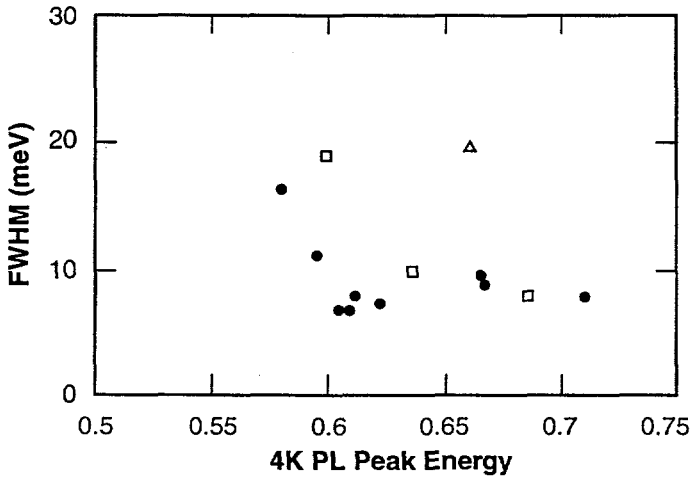

304549-10

Figure 5

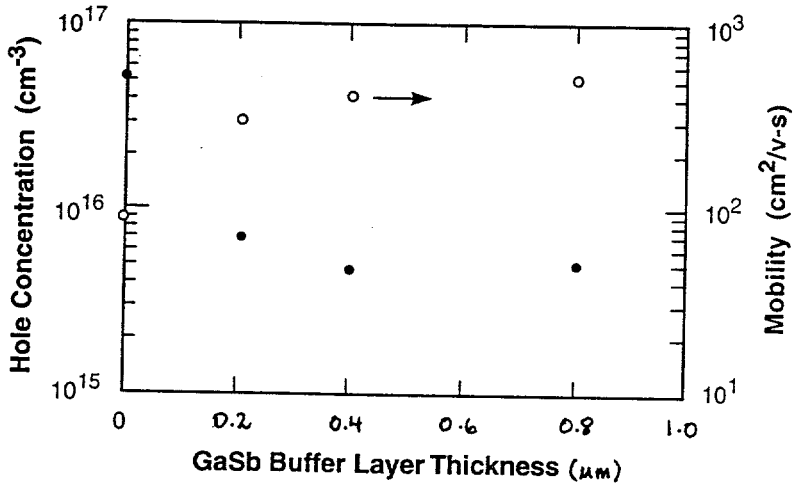

304549-2

Figure 6

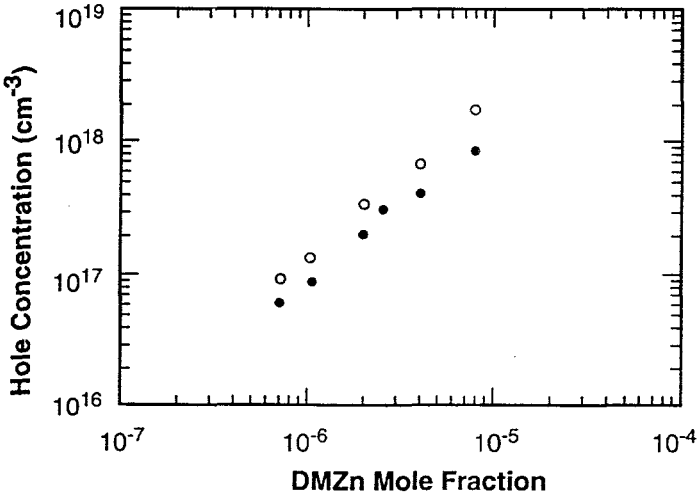

304549-9

Figure 7a

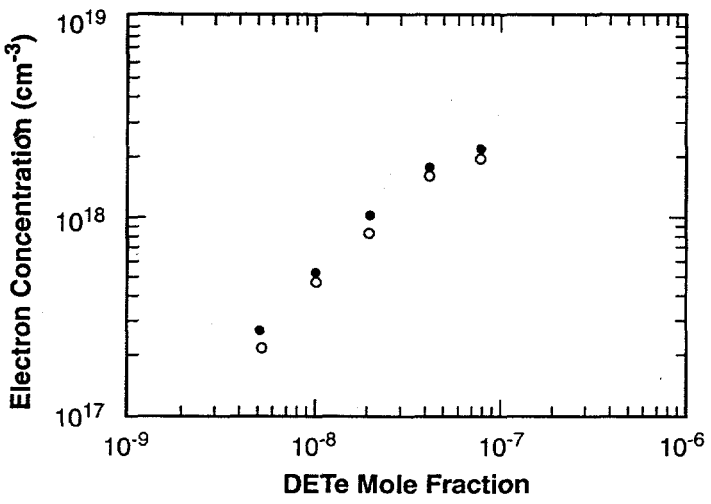

304549-8

Figure 7b

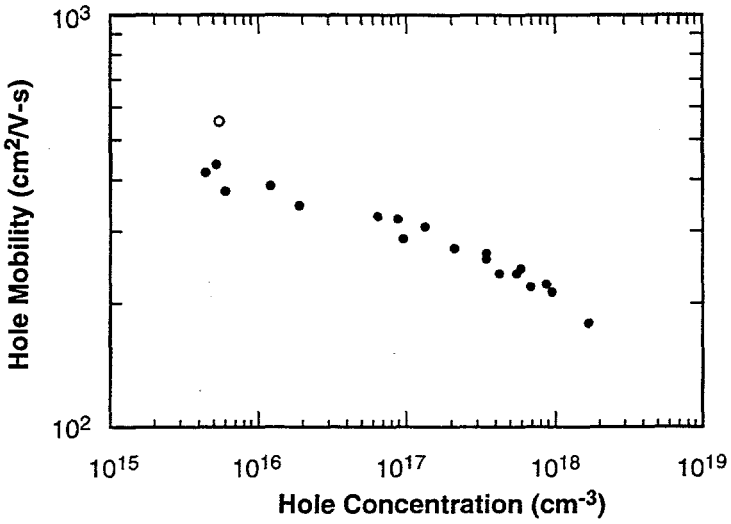

304549-4

Figure 8a

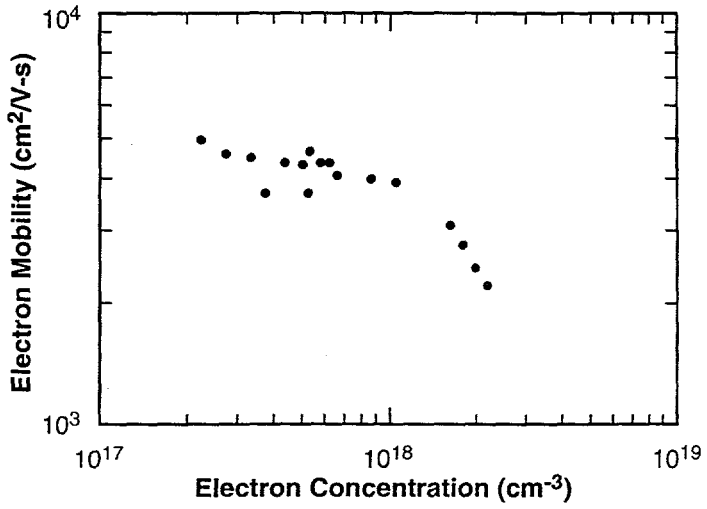

Figure 8b